

Anomalous transport on polymeric porous film electrodes in the dopant-induced insulator-to-conductor transition analyzed by electrochemical impedance

Germà Garcia-Belmonte^{a)} and Juan Bisquert

Departament de Ciències Experimentals, Universitat Jaume I, E-12080 Castelló, Spain

Ernesto C. Pereira

Laboratório Interdisciplinar de Eletroquímica e Cerâmica-Departamento de Química, Universidade Federal de São Carlos, P.O. Box 676, 13560-905 São Carlos, SP Brazil

Francisco Fabregat-Santiago

Departament de Ciències Experimentals, Universitat Jaume I, E-12080 Castelló, Spain

(Received 31 May 2000; accepted for publication 16 January 2001)

In the present letter, we have identified anomalous transport patterns on conducting polymer thin-film electrodes [poly(thiophene-3-acetic acid)] by means of electrochemical impedance measurements. This type of electrical behavior yields conductance responses exhibiting frequency dispersion at frequencies in excess of the ac onset ω_c . The study of impedance spectra under variation of the applied potential allows to determine the threshold potential at which a dopant-induced insulator-to-conductor transition takes place. Moreover, since the charge carrier concentration in the polymer matrix is directly modulated by the insertion of anions via the applied potential, some relevant aspects of the doping process, such as the dimensionality of the ion insertion, can be properly investigated. © 2001 American Institute of Physics.
[DOI: 10.1063/1.1354671]

Charge transport mechanisms in conducting polymers, although extensively studied over the past two decades, are still far from being completely understood. At the phenomenological level of description, the conductivity of ion-doped polymers usually displays a crossover from a dc value $\sigma(0)$ to a power law regime at high frequencies given by

$$\begin{aligned}\sigma(\omega) &= \sigma(0), & \omega \ll \omega_c, \\ \sigma(\omega) &\propto \omega^s, & \omega \gg \omega_c,\end{aligned}\quad (1)$$

where ω_c is the crossover frequency that marks the onset of the ac conductivity, and s ($0.6 < s < 0.9$) corresponds to the power-law exponent in this regime.^{1,2} Conduction is believed to take place by means of polaron-type particles³⁻⁷ (polarons, bipolarons or also polaron clusters) and, therefore, variable-range hopping models have provided fruitful outcomes.⁸ However, it is widely acknowledged that structural effects may strongly influence the observed macroscopic electrical response. The structural disposition of the polymeric strands (crystalline or amorphous polymers), the length of the polymer chains, and also the possible disordered location of anions during the doping process are, among others, determining aspects of the conducting mechanism. Some authors have even argued that disorder effects completely mask the original features of polarons because transport processes average out most of the microscopic details.⁹⁻¹¹ In all, wide agreement appears to exist in regarding hopping as the underlying transport mechanism, and this fact should be phenomenologically represented in terms of conductivity by expressions like Eq. (1).

While the solid-state physics approach has established the generality of the conductivity response introduced, the frequency dependence of the conductivity has been largely disregarded in the electrochemical approaches, which usually model the effect of the polymer conduction on the response of the electrochemical cell by means of a simple resistor element. There are two principal approaches to modeling the impedance response of polymer electrodes. One of them assumes a uniform, homogeneous film,^{12,13} while the other takes into account the intrinsic porous structure.^{14,15} In such electrodes, polymer chains form a tangled structure, which allows the presence of pores inside the film and also opened to the electrolyte.¹⁶ Porosity usually yields an additional degree of disorder.

In a recent paper¹⁷ we have theoretically studied the repercussion of the frequency dependence of the conductivity on the electrochemical impedance of porous film electrodes. Among the available models for analyzing these electrochemical devices, the more fruitful approach is based on a doubled-channel electrical transmission line impedance models.^{15,18-23} These models respect the distributed character of the electrical effects because of porosity. Each phase is represented by means of an electrical element that accounts for its specific behavior. In the simplest, and therefore formally tractable, model only three elements are needed: (a) a subcircuit for the electroactive solid matrix, (b) a resistive element for the electrolyte inside the pores, and (c) a capacitive-like one for the distributed inner contact between the polymer and the electrolyte. It has been demonstrated¹⁷ that the first dominates the electrical response of the whole electrochemical cell in certain circumstances and high frequencies, especially when the polymer is kept in its dopant-

^{a)}Author to whom correspondence should be addressed; electronic mail: garciag@uji.es

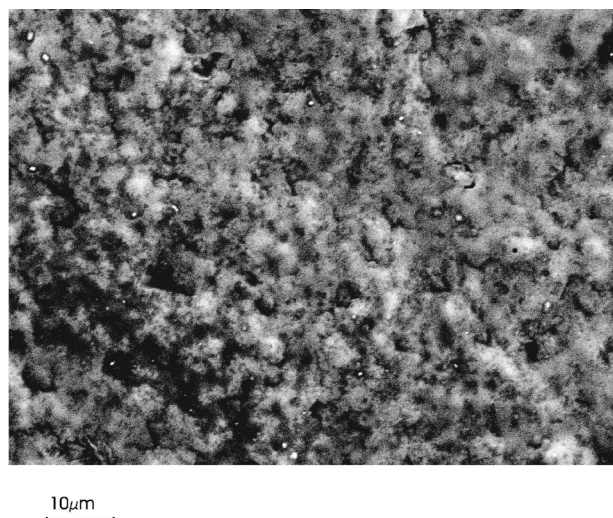


FIG. 1. Scanning electron microscopy image of the [poly(thiophene-3-acetic acid)] film in its reduced state.

induced conducting (oxidized) state or near the insulator to conductor transition.

We have analyzed the electrical properties of a porous film comprised of [poly(thiophene-3-acetic acid)] using electrochemical impedance. The synthesis of the polymer was carried out in the presence of FeCl_3 in a CHCl_3 medium using 0.01 M monomer and 0.05 M oxidant. (see Refs. 23 and 24 for more synthesis details). The working electrodes were polymer films deposited on Pt plates (surface area 1.4 cm^2 and estimated thickness $10 \mu\text{m}$) by casting from N,N-dimethylformamide solution. With the aim of verifying the actual porous nature, we obtained scanning electron microscopy images of these films. Figure 1 shows a very irregular electrode surface, on which pores (black zones in the image) are clearly visible. The size of these pores ranges approximately from 1 up to $5 \mu\text{m}$.

The impedance spectroscopy measurements were made in the frequency range from 10 kHz down to 1 mHz, using an ac voltage of 10 mV root-mean-square at different dc potentials. A FRA Solartron model 1260 coupled to the potentiostat were employed in the experiments. With the aim of achieving a homogeneous distribution of the doping anions, we assured the cell to reach the electrochemical steady state (current reaches near zero values) waiting 30 min between the application of the dc potential and the data recording. Impedance measurements under variation of the applied, steady state potential are plotted in Fig. 2. A general view [Fig. 2(a)], which shows the response in the whole frequency window, displays the electrical contribution of all the cell elements on the impedance. However, if we restrict the observed range to the high-frequency wing [Fig. 2(b)], depressed arcs corresponding to the polymer electrical effect are clearly distinguishable. As general trends, the associated resistance of this process increases when the applied potential decreases. Examination of the high frequency intercept of the impedance plots with the real axis [Fig. 2(b)] shows that all of them coincide in the same point. This evidently must be related to the uncompensated resistance of the electrolyte outside the film. The common intercept reinforces the idea that the high-frequency arc reflects the conducting be-

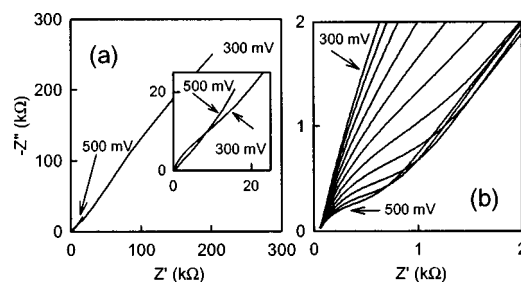


FIG. 2. Impedance spectra of [poly(thiophene-3-acetic acid)] under variation of the applied potential. (a) Overall response for reduced (300 mV) and oxidized (500 mV) polymer states. (b) High frequency wing detail (increasing 20 mV between each spectrum).

havior of the polymer. As several detailed analysis have shown,^{15,20} this high frequency intercept varies as a function of the applied potential in the case of mixed conduction effects due to nondispersive transport in the polymeric matrix and ionic transport in the electrolyte.

In terms of circuit elements, a depressed arc in an impedance plot may be represented by the parallel combination of a resistance R and a constant-phase element (CPE) with impedance:

$$Z_{\text{CPE}}(\omega) = \frac{1}{Q(i\omega)^s}. \quad (2)$$

The admittance of the parallel combination will be thus given by the following expression:

$$Y(\omega) = R^{-1} + Q(i\omega)^s \quad (3)$$

and, taking into account that the real part of the admittance directly corresponds to the conductance $G(\omega)$, we obtain an expression compatible with that of Eq. (1),

$$G(\omega) = G(0)[1 + (\omega/\omega_c)^s], \quad (4)$$

in which we have performed the following identifications:

$$G(0) = R^{-1}, \quad (5)$$

$$\omega_c = \left[\frac{1}{RQ \sin(s\pi/2)} \right]^{1/s}. \quad (6)$$

Some remarks may be made about the capacitive effect of the CPE. On one hand, the impedance corresponding to Eq. (3) displays an imaginary part that increases for frequencies in excess of ω_c and this provokes the occurrence of frequency dispersion on capacitance. Obviously, since $C(\omega) = Y''(\omega)/i\omega$, a power law of frequency appears as $C(\omega) \propto \omega^{-(1-s)}$. This type of capacitive behavior was adequately observed by Glarum and Marshall²⁵ in their study on polyaniline electrode films, although an ionic rather than electronic (polaronic) origin was attributed in that work.

Other types of capacitive effects are, in addition, possible. It was suggested that these may arise from the high frequency polarizability²¹ of the polymer and also from the imbalance of charge related to electron hopping from one polymer strand to another. With respect to the first possibility, it is evident that its effect must lie at frequencies higher than the limit of the measurement window situated at 10 kHz. The second effect was analyzed by Alberly and Mount,²⁶ rejecting its occurrence from their measurements on polypyrrole as a conclusion.

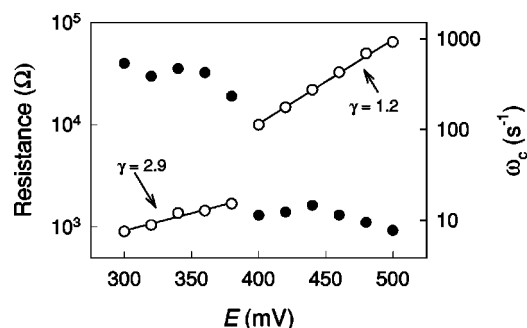


FIG. 3. (a) (●) Polymer resistance R as a function of the applied potential E , obtained from fits of the high-frequency wing of the impedance spectra. Note the sharp variation at ~ 390 mV that marks the insulator-to-conductor transition. (b) (○) Crossover frequency ω_c under variation of the applied potential. Dimensionality of the doping process γ has been calculated for the reduced (300–380 mV) and oxidized (400–500 mV) states.

We have fitted the high frequency wing of the impedance plots using a nonlinear least-square algorithm with the equivalent circuit resulting from Eq. (3), plus a resistance in series accounting for the uncompensated electrolyte. In curve (a) of Fig. 3 the polymer resistance R is plotted as a function of the applied potential. The insulator-to-conductor transition is apparent in the sharp resistance variation that marks the onset of the oxidized state of the polymer. This has been interpreted in terms of a threshold potential E_{th} at which the growth of conducting regions inside the polymer matrix provides conducting paths of the size of the film thickness.^{27–29}

Aiming to explore more deeply the variation ω_c with the applied potential, it is useful to recall that in the framework of anomalous diffusion this crossover frequency signals the size ξ of some type of clustering spatial structure. This is the case of percolation clusters,^{30,31} in which ω_c indicates the correlation length of the cluster. Assuming that conduction takes place by hopping between available locations, the characteristic size related to ω_c should decrease as the concentration n of charge carrier increases. This concentration is obviously modulated by the insertion of anions during doping. Therefore, the next chain of proportions^{32,33} holds $\omega_c \propto \xi^{-2} \propto n^{2/3\gamma}$, where γ accounts for the dimensionality of the doping process with $\gamma=1$ for three-dimensional insertion or $\gamma=2$ for a two-dimensional one. As is common in electrochemical reactions, the charge carrier concentration (now related to anion concentration) is modulated by the overpotential E following an exponential relation: $n \propto \exp(E/kT)$, k being the Boltzmann constant and T the absolute temperature. Finally, identifying E with the applied potential, the slope of the following expression provides additional information on charge carrier distribution,

$$\ln \omega_c \propto \frac{2}{3\gamma} \frac{E}{kT}. \quad (7)$$

Curve (b) in Fig. 3 plots the variation of ω_c with the applied potential. It is observed that near E_{th} the dependence does not correspond to that proposed in Eq. (7). This could be explained because at this potential the films undergo significant morphological changes: the volume occupied by the

films grows drastically, presumably due to the repulsive interaction of the increasing number of located anions. However, at both low and high potential linear correlations are displayed in curve (b) of Fig. 3. For the reduced state region, γ results approximately equal to 2.9, thus indicating that the dimensionality of doping lies near 1. Therefore, only few directions participate in the doping that advances slowly. On the other hand, when the film switches to the oxidized state, $\gamma=1.2$. This result shows that doping takes place over many, practically three-dimensional, available directions. In all, this value for γ suggests that the polymeric film does not fill all the space, precisely because of the porous complex structure.

La Comisión Interministerial de Ciencia y Tecnología of Spanish Government is acknowledged for supporting these studies under Projects MAT98-0342 and PB98-1045.

- ¹S. K. Saha, T. K. Mandal, B. M. Mandal, and D. Chakravorty, *J. Appl. Phys.* **81**, 2646 (1997).
- ²J. A. Reedijk, H. C. F. Martens, H. B. Brom, and M. A. J. Michels, *Phys. Rev. Lett.* **83**, 3904 (1999).
- ³S. Ramadhar, R. P. Tandon, and S. Chandra, *J. Phys.: Condens. Matter* **5**, 1313 (1993).
- ⁴A. A. Zakhidov, T. Akashi, and K. Yoshino, *Synth. Met.* **70**, 1519 (1995).
- ⁵I. A. Howard and J. L. Rhodes, *Synth. Met.* **58**, 195 (1993).
- ⁶L. B. Schein and J. X. Mack, *Chem. Phys. Lett.* **149**, 109 (1988).
- ⁷A. Saxena and J. D. Gunton, *Phys. Rev. B* **35**, 3914 (1987).
- ⁸J. Joo, S. M. Long, J. P. Pouget, E. J. Oh, A. G. MacDiarmid, and A. J. Epstein, *Phys. Rev. B* **57**, 9567 (1998).
- ⁹P. M. Borsenberger, L. Pautmeier, and H. Bässler, *J. Chem. Phys.* **94**, 5447 (1991).
- ¹⁰H. Bässler, *Phys. Status Solidi B* **175**, 15 (1993).
- ¹¹H. Bässler, P. M. Borsenberger, and R. J. Perry, *J. Polym. Sci., Polym. Phys.* **32**, 1677 (1994).
- ¹²M. A. Vorotyntsev, C. Deslouis, M. M. Musiani, B. Tribollet, and K. Aoki, *Electrochim. Acta* **44**, 2105 (1999).
- ¹³G. Láng and G. Inzelt, *Electrochim. Acta* **44**, 2037 (1999).
- ¹⁴S. Fletcher, *J. Chem. Soc., Faraday Trans.* **89**, 311 (1993).
- ¹⁵K. Rossberg, G. Paasch, L. Dunsch, and S. Ludwig, *J. Electroanal. Chem.* **443**, 49 (1998).
- ¹⁶T. F. Otero, H. Grande, and J. Rodriguez, *J. Electroanal. Chem.* **394**, 211 (1995).
- ¹⁷J. Bisquert, G. Garcia-Belmonte, F. Fabregat-Santiago, and A. Compte, *Electrochem. Commun.* **1**, 429 (1999).
- ¹⁸W. J. Albery and A. R. Mount, *J. Chem. Soc., Faraday Trans.* **90**, 1115 (1994).
- ¹⁹R. de Levie, *Electrochim. Acta* **8**, 751 (1963).
- ²⁰X. Ren and P. G. Pickup, *J. Chem. Soc., Faraday Trans.* **89**, 321 (1993).
- ²¹S. Fletcher, *J. Electroanal. Chem.* **337**, 127 (1992).
- ²²J. Bisquert, G. Garcia-Belmonte, F. Fabregat-Santiago, N. S. Ferriols, P. Bogdanoff, and E. C. Pereira, *J. Phys. Chem.* **104**, 2287 (2000).
- ²³J. Bisquert, G. Garcia-Belmonte, F. Fabregat-Santiago, N. S. Ferriols, M. Yamashita, and E. C. Pereira, *Electrochem. Commun.* **2**, 601 (2000).
- ²⁴G. Garcia-Belmonte, J. Bisquert, F. Fabregat-Santiago, M. Yamashita, and E. C. Pereira, *Ionics* **5**, 44 (1999).
- ²⁵S. H. Glarum and J. H. Marshall, *J. Electrochem. Soc.* **134**, 142 (1987).
- ²⁶W. J. Albery and A. R. Mount, *J. Electroanal. Chem.* **305**, 3 (1991).
- ²⁷Y. Teragishi and K. Aoki, *J. Electroanal. Chem.* **473**, 132 (1999).
- ²⁸Y. Tezuka, K. Aoki, H. Yajima, and T. Ishii, *J. Electroanal. Chem.* **425**, 167 (1997).
- ²⁹K. Aoki and M. Kawase, *J. Electroanal. Chem.* **377**, 125 (1994).
- ³⁰G. A. Niklasson, *J. Appl. Phys.* **62**, R1 (1987).
- ³¹A. N. Samukhin, P. V. N. L. Jastrabik, and A. J. Epstein, *Phys. Rev. B* **58**, 11354 (1998).
- ³²D. L. Sidebottom, *Phys. Rev. Lett.* **83**, 983 (1999).
- ³³D. L. Sidebottom, P. F. Green, and R. K. Brow, *Phys. Rev. B* **56**, 170 (1997).